The Journal of Supercritical Fluids 143 (2019) 370–377

Contents lists available at ScienceDirect

The Journal of Supercritical Fluids

journal homepage: www.elsevier.com/locate/supflu

Determination of retro-aldol reaction type for glyceraldehyde under hydrothermal conditions

Rahmat Iman Mainil[a,b], Nattacha Paksung[a], Yukihiko Matsumura[a,*]

[a] Department of Mechanical Science and Engineering, Hiroshima University, 1-4-1 Kagamiyama, Higashi-Hiroshima, 739-8527, Japan
[b] Department of Mechanical Engineering, Universitas Riau, Pekanbaru, Riau, Indonesia

GRAPHICAL ABSTRACT

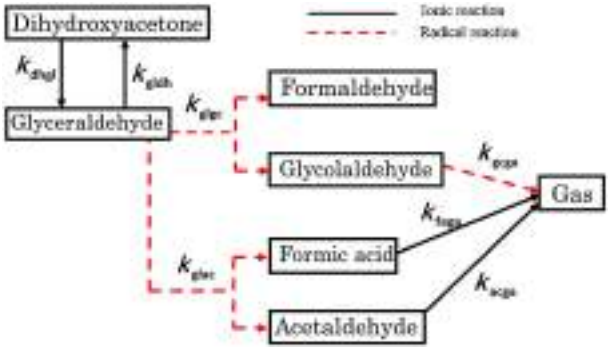

ARTICLE INFO

Keywords:
Glyceraldehydee
Supercritical water
Radical reaction
Reaction kinetics

ABSTRACT

Whether the retro-aldol reaction observed in the treatment of sugar molecules with hot compressed water occurs via an ionic or a radical reaction remains an open question. Conventionally, the retro-aldol reaction is a known ionic reaction. However, recent experiments performed under hydrothermal conditions have shown that the retro-aldol reaction occurs via a radical reaction. In this work, glyceraldehyde, the simplest sugar to undergo retro-aldol reaction, is used to clearly demonstrate that the retro-aldol reaction of glyceraldehyde under hydrothermal conditions is a radical reaction. Glyceraldehyde was dissolved in deionized water and then heated to 350–450 °C at a fixed pressure of 25 MPa in a continuous reactor. The reaction rate of glyceraldehyde followed Arrhenius's Law, irrespective of subcritical or supercritical temperatures. The reaction network of glyceraldehyde was also developed and each reaction rate was determined.

1. Introduction

Increasing energy demands, fossil fuel depletion, and environmental degradation are some of the issues that motivate the search for renewable energy sources. Biomass is an alternative energy source, which is abundant, carbon neutral, and environmentally friendly [1,2]. Supercritical water gasification (SCWG) is a high-potential technology to convert biomass into energy via its transformation into value-added fuel gas. In this technology, water functions as both the reactant and reaction medium. Many organic compounds and gases can be easily dissolved in supercritical water as it behaves like an organic solvent [3–5]. This is owing to the decreased dielectric constant of water under certain conditions, which in turn results in decreased water density and weakening of the hydrogen bonds between the water molecules. As

* Corresponding author.
E-mail address: mat@hiroshima-u.ac.jp (Y. Matsumura).

https://doi.org/10.1016/j.supflu.2018.09.013
Received 14 June 2018; Received in revised form 24 September 2018; Accepted 24 September 2018
Available online 26 September 2018

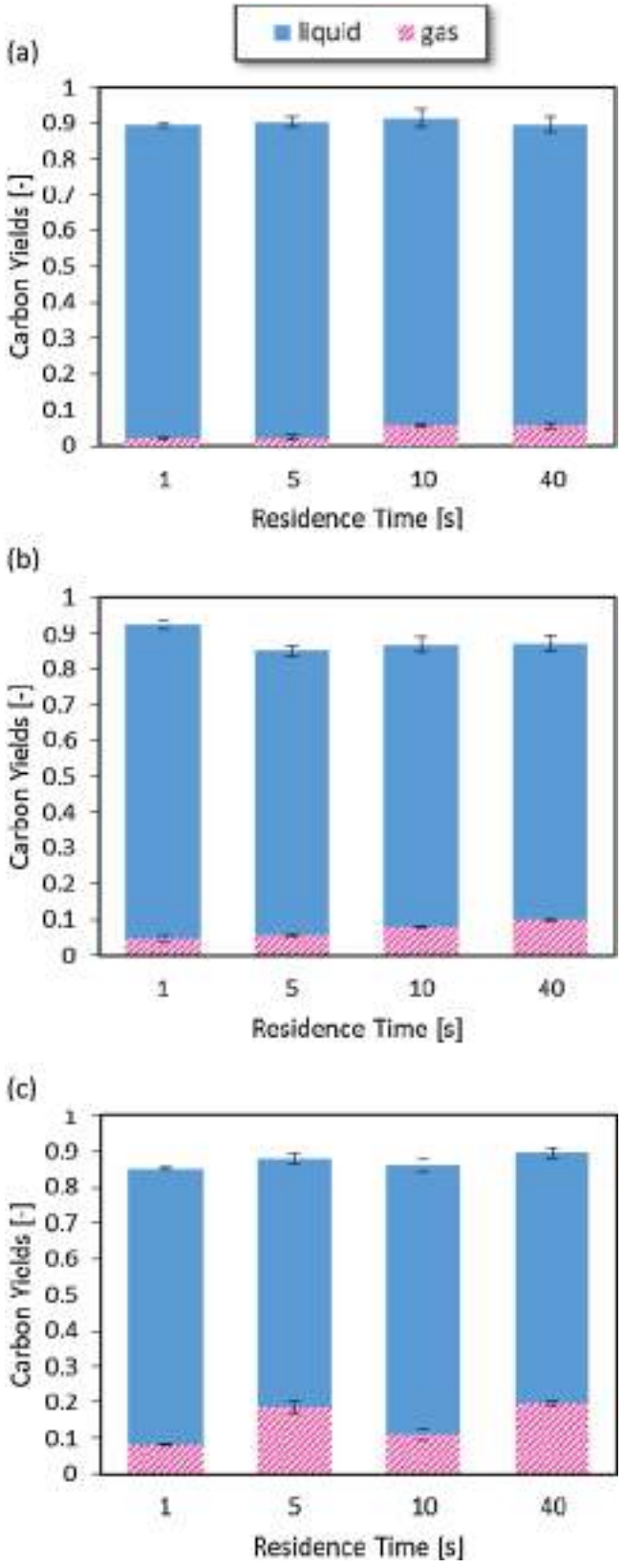

Fig. 1. Carbon yields of glyceraldehyde conversion at reaction temperatures of (a) 350 °C, (b) 400 °C, (c) 450 °C.

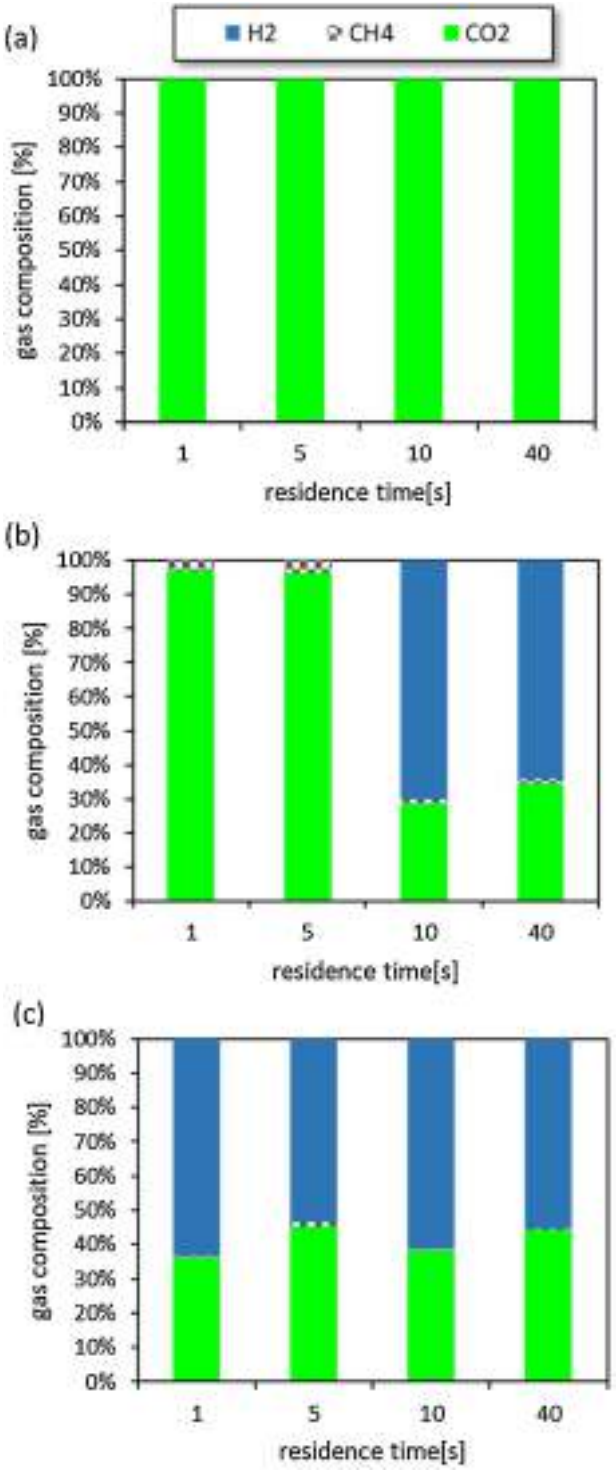

Fig. 2. Gas compositions of glyceraldehyde decomposition at reaction temperatures of (a) 350 °C, (b) 400 °C, (c) 450 °C.

consequence, the biomass will be easily gasified [6–9]. This excellent capability occurs at high temperatures and high pressures above the critical point of water (374 °C and 22.1 MPa, respectively) [10,11].

Many researchers have investigated the decomposition of model compounds by SCWG. These compounds are effective for understanding the reaction characteristics of biomass. Glucose, a model compound of cellulose, has been widely studied in terms of its decomposition behavior in hot compressed water. The reaction kinetics of glucose at very short residence times have been reported by Kabyemela et al. [12] In their study, several intermediate compounds were identified as the decomposition products at temperatures of 300–400 °C. A reaction network model was developed to correlate the differential equations of

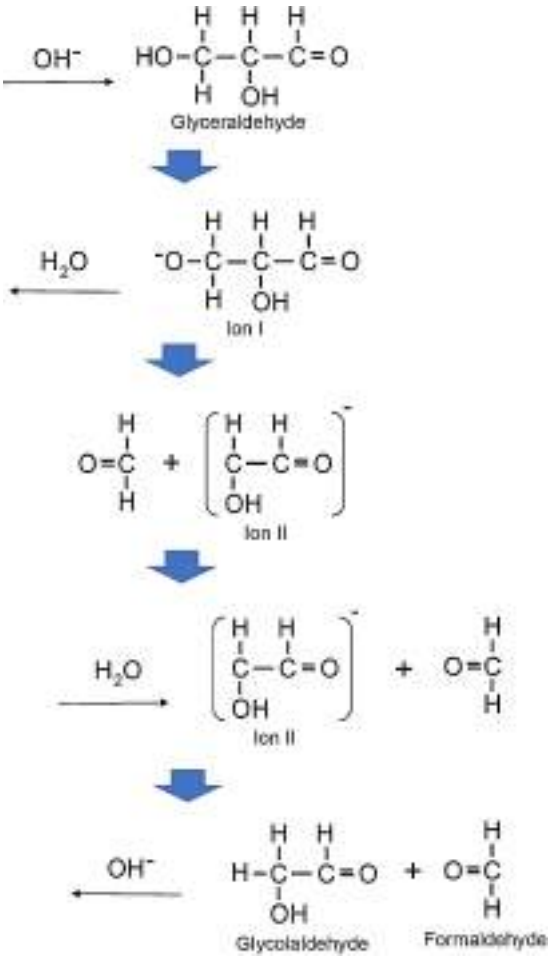

Fig. 3. Mechanism of glyceraldehyde decomposition by ionic reaction.

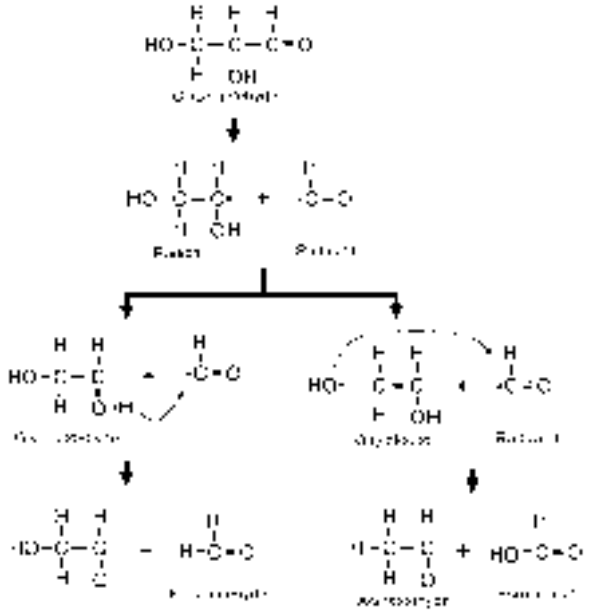

Fig. 4. Mechanism of glyceraldehyde decomposition by radical reaction.

the reaction pathways and experimental results. Promdej and Matsumura [13] evaluated the glucose conversion behavior in sub- and supercritical water. The effect of temperature was successfully employed to classify the reactions into either ionic or radical. Namely, certain reactions were retarded at supercritical temperatures, deviating from the Arrhenius Law. This behavior was explained by the instability of generated ions in supercritical water owing to the decrease in the dielectric constant. Thus, the reaction rates of the ionic reactions were lowered in the supercritical region, whereas the reaction rates of the radical reactions followed Arrhenius' Law irrespective of the use of sub- or supercritical water. Aida et al. reported on the reaction kinetics of D-xylose in sub- and supercritical water [14]. D-xylose and the retro-aldol reaction products were the primary intermediates observed under these experimental conditions, and their kinetic rate constants depended on the reaction pressure. Goodwin and Rorrer presented the gasification of the model compound xylose in supercritical water [8,15]. A microchannel reactor was used to obtain high heat transfer rates, resulting in enhanced gasification. Our research group elucidated the detailed mechanisms of xylose decomposition in both sub- and supercritical water [16,17]. It was clearly shown that the formic acid and total organic carbon present in the liquid effluents were gasified, whereas acetic acid and formaldehyde were not gasified at the temperatures investigated. The effect of temperature was also used to classify the reactions into ionic or free radical reactions.

One of the mysteries that still exists with respect to sugar treatment under hydrothermal conditions, however, is whether the retro-aldol reaction is an ionic or a radical reaction. From the decomposition studies of glucose, reverse-aldol condensation reactions occur during SCWG [3,18]. Conventionally, the aldol condensation and, thus, its reverse reaction, the retro-aldol reaction, are well-known ionic reactions. However, experiments under hydrothermal conditions have shown that the retro-aldol reaction occurs via a radical reaction for glucose [13] and xylose [16,17]. Furthermore, the complexity of the reaction networks, numerous reaction products, and unstable intermediates prohibit the detailed studies of these reactions.

To elucidate the nature of the reaction mechanism occurring during the retro-aldol reaction of sugars under hydrothermal conditions, the use of simple sugars should be effective. Glyceraldehyde, a triose monosaccharide with the chemical formula $C_3H_6O_3$, is the simplest aldol sugar that can undergo retro-aldol reaction and is therefore suitable for this purpose. Thus far, only Honma and Inomata have attempted to elucidate glyceraldehyde conversion in supercritical water [19]. However, their study was non-empirical; they performed calculations using the density functional theory. To the best of our knowledge, there are no comprehensive experimental studies on glyceraldehyde conversion in sub- and/or supercritical water from which the

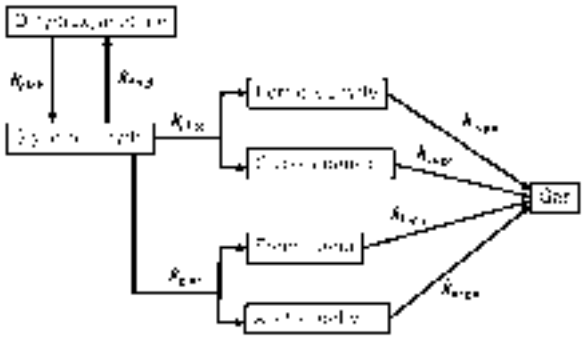

Fig. 5. Reaction network for glyceraldehyde decomposition.

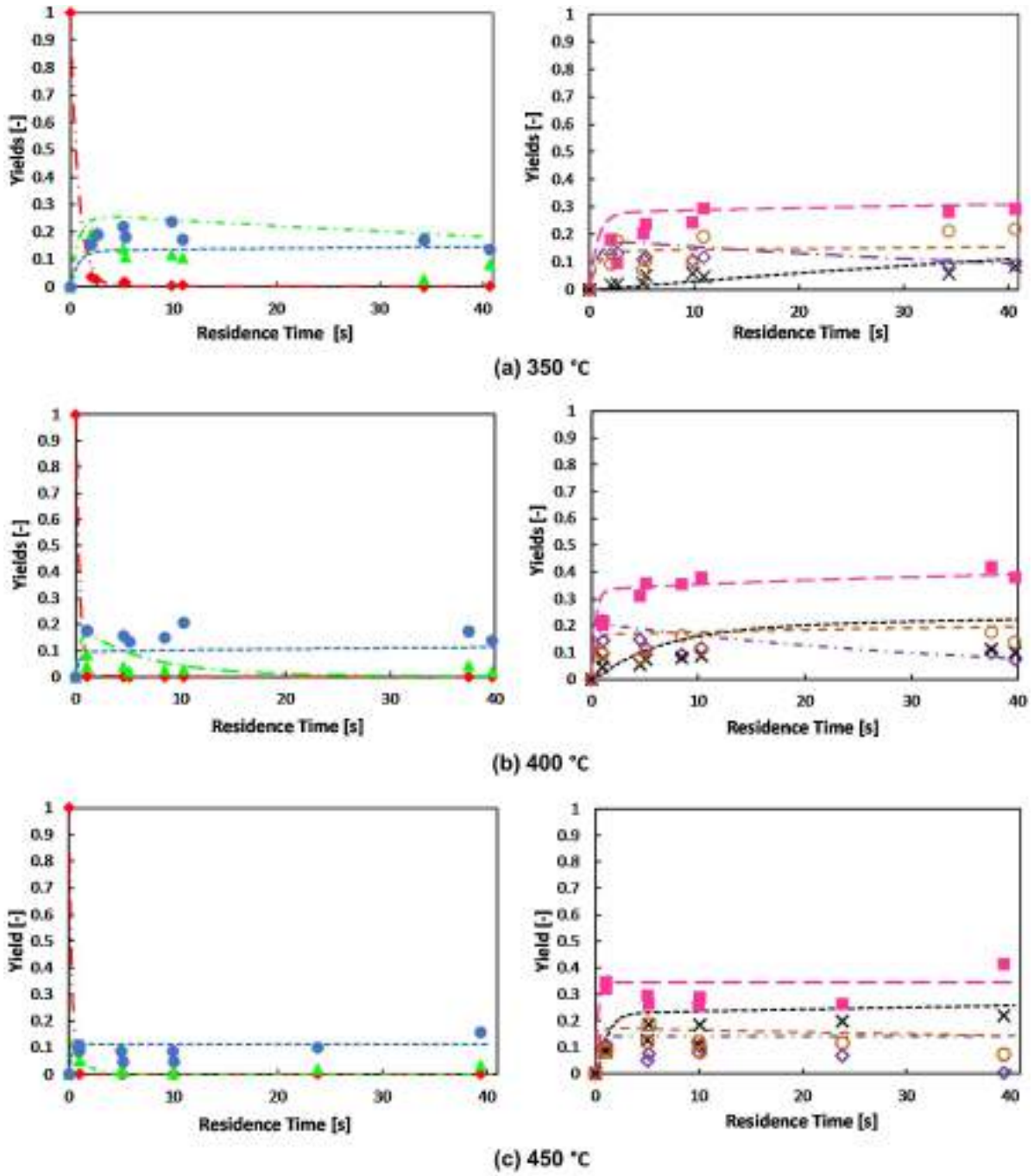

Fig. 6. Effect of temperature and residence time on behavior of glyceraldehyde conversion at temperatures (a) 350 °C, (b) 400 °C, (c) 450 °C. Symbols: ◆= glyceraldehyde, ● = formaldehyde, ▲= glycolaldehyde, ◇= dihydroxyacetone, ■ = acetaldehyde, ○= formic acid, ✕= gas, –·–= calculation of glyceraldehyde, ▬▬▬▬▬= calculation of formaldehyde, ···= calculation of glycolaldehyde, –··– = calculation of dihydroxyacetone, – – = calculation of acetaldehyde, - - - = calculation of formic acid, -----= calculation of gas.

detailed reaction mechanisms and reaction kinetics can be elucidated. Therefore, in this study, we will investigate the kinetics of glyceraldehyde decomposition under hydrothermal conditions to shed light on the mechanism(s) of the retro-aldol reaction of sugars under hydrothermal conditions.

2. Experimental section

The experiments were conducted using a continuous stainless-steel (SS316) reactor with inner and outer diameters of 1 and 1.59 mm, respectively. The reactor was equipped with a preheater, heat exchanger, high-pressure pumps, a back-pressure regulator, and a gas and liquid sampling port. The schematic of the experimental apparatus and details of the reactor operating procedure have been presented elsewhere [20]. In brief, a 0.5 wt% concentration of the feedstock solution (glyceraldehyde obtained from Nacalai Tesque Co., purity 98%) was fed into the reactor where it was mixed with preheated water at a ratio of 1:4 to give a 0.1 wt% diluted reaction solution. The back-pressure regulator ensured that the reaction was maintained at a constant pressure of 25 MPa. The reaction temperature was varied from 350 to

Table 1
Kinetic parameters value of each reactions in reaction pathways of glyceraldehysde decomposition under sub and supercritical conditions.

Kinetic Parameter	Reaction	k [s^{-1}]		
		350 °C	400 °C	450 °C
k_{glgc}	Retro-aldol reaction	5.10×10^{-1}	7.97×10^{-1}	1.20×10^{0}
k_{gldh}	Isomerization	2.33×10^{-1}	5.75×10^{-1}	4.97×10^{-1}
k_{dhgl}	Isomerization	2.02×10^{-2}	3.23×10^{-2}	0.00×10^{0}
k_{glac}	Decomposition	5.39×10^{-1}	1.38×10^{0}	1.83×10^{0}
k_{gcga}	Gasification	1.26×10^{-2}	1.68×10^{1}	1.17×10^{0}
k_{foga}	Gasification	0.00×10^{0}	0.00×10^{0}	0.00×10^{0}
k_{faga}	Gasification	0.00×10^{0}	0.00×10^{0}	4.76×10^{-3}
k_{acga}	Gasification	0.00×10^{0}	0.00×10^{0}	0.00×10^{0}
k_x	Total glyceraldehyde decomposition	1.31×10^{0}	2.95×10^{0}	4.7×10^{0}

450 °C to accommodate both sub- and supercritical conditions. Different residence times (1, 5, 10, and 40 s) were obtained by controlling the flow rate. To terminate the reaction, the product effluent discharged from the reactor exit was immediately mixed with room temperature water. The solid products if any were trapped inside the inline filters, allowing the liquid and gas products to be collected at the sampling ports.

The liquid effluent was analyzed using a total organic carbon (TOC) analyzer. This apparatus quantifies both the amount of carbon present in the liquid phase (non-purgeable organic carbon) as well as the dissolved carbon dioxide (inorganic carbon). High-performance liquid chromatography (HPLC) was employed to determine the compounds in the liquid with the aid of the appropriate methods and standards. For analyzing the glyceraldehyde and the retro-aldol products (formaldehyde, glycolaldehyde, and acetaldehyde), a SCR102H column (Shimadzu) was used with a 0.005 M $HClO_4$ aqueous solution as the mobile phase. This column was operated with a flow rate of 0.7 mL/min, an oven temperature 40 °C, and a refractive index detector (RID). A K108 column (Shodex) with deionized water as the mobile phase (flow rate 0.7 mL/min; oven temperature 60 °C, RID) was used for determining the dihydroxyacetone content.

The gaseous products were quantitatively analyzed using gas chromatography (GC). The GC was equipped with a flame ionization detector (FID), and He was used as the carrier gas to detect CH_4, C_2H_2, and C_2H_6. A thermal conductivity detector (TCD) employing He as the carrier gas was used to detect CO_2 and CO. The TCD was also used to detect H_2 gas with N_2 as the carrier gas.

The product yields from glyceraldehyde decomposition were calculated based on the carbon amount using the following equation:

$$(\text{Carbon yield } [-]) = \frac{(\text{Carbon in product [mg-C/min]})}{(\text{Carbon in feedstock [mg-C/min]})} \quad (1)$$

3. Results and discussion

3.1. Product yields of gaseous and liquid products

To study the reaction mechanism of the retro-aldol reaction of glyceraldehyde under hydrothermal conditions, the effects of temperature and reaction time on the yields of the liquid and gaseous products were first studied. Both temperature and time significantly affected the nature of the products obtained. Fig. 1 clearly shows that the carbon yield of the gaseous products was lower than that of liquid products at all temperatures (350–450 °C) and residence times. Gas production increased with temperature, similar to previous reports by Lu et al. [21]. This was due to the decrease in the density of the water with increasing temperature, which led to the suppression of ionic products and, subsequently, the domination of the free radical reactions. Moreover, longer reaction times also resulted in increased gas production yields. This too was in good agreement with previous research [16]. The formation of solid products was rarely obtained in this work and was, therefore, neglected from further considerations. The carbon balance of each experiment was higher than 0.85, confirming the reliability of the data.

Fig. 2 shows the product gas composition. Temperature had significant effect on the product gas composition. The gas products were mainly composed of CO_2, H_2, and small amount of CH_4. At temperature of 350 °C, only CO_2 was observed for all reaction times. At higer temperature 400 and 450 °C, H_2 started to be formed and small quantities of CH_4 was found.

3.2. Mechanism of glyceraldehyde decomposition

Glyceraldehyde is a monosaccharide with the chemical formula $C_3H_6O_3$. It possesses one carbonyl group and two hydroxyl groups, one primary and one secondary. It is the simplest aldose [22]. Furthermore, it is known that when monosaccharides are treated with supercritical water, retro-aldol reaction occurs [23] in addition to isomerization.

As explained previously, the retro-aldol reaction is a well-known ionic reaction. A typical reaction scheme based on the well-taught mechanisms found in organic chemistry textbooks is shown in Fig. 3. The retro-aldol reaction of glyceraldehyde produces glycolaldehyde and formaldehyde. In the first step, the hydroxide ion abstracts a hydrogen ion from the glyceraldehyde molecule. The resulting ion **I** subsequently dissociates to give formaldehyde and ion **II**. Finally, ion **II** abstracts a hydrogen ion from water, forming glycolaldehyde, and the hydroxide ion is regenerated.

As shown in Fig. 4, however, the same products are also obtained via the radical reaction mechanism. Glyceraldehyde dissociates into radical **I** and radical **II**. The former is converted into 1,2-dihydroxyethene by releasing a hydrogen radical. This hydrogen radical reacts with radical **II** to form formaldehyde. Meanwhile, keto-enol tautomerization converts 1,2-dihydroxyethene into glycol aldehyde. It should be noted that radical **I** can also be converted into vinyl alcohol by releasing a hydroxyl radical. In this case, the hydroxyl radical reacts with radical **II** to form formic acid and vinyl alcohol is converted into acetaldehyde.

To determine which of these mechanisms is correct, a change in the reaction rate with temperature was exploited. If the reaction rate decreased in the supercritical region, it would be because of the decreasing stability of the associated ions, and thus it could be inferred that an ionic reaction occurred. However, if the reaction rate follows the Arrhenius law, it would imply that the associated intermediates are not ions, indicating a radical reaction mechanism. Furthermore, in the case of the radical reaction, formic acid is produced. This is not the case for the ionic reaction.

3.3. Kinetic model of glyceraldehyde decompositions

Based on the mechanisms shown in Figs. 3 and 4, the reaction network shown in Fig. 5 can be applied. Accordingly, a set of differential equations for glyceraldehyde conversion can be developed (Eqs. (2)–(8)), from which the reaction rates can be evaluated. This set of differential equations encompasses also the production of formic acid and acetaldehyde, whose reaction rates should be zero for the case of the ionic reactions.

$$\frac{dY_c(glyceraldehyde)}{dt} = k_{dhgl}Y_c(dihydroxyacetone) - (k_{glgc} + k_{gldh} + k_{glac})Y_c(glyceraldehyde) \quad (2)$$

$$\frac{dY_c(dihydroxyacetone)}{dt} = k_{gldh}Y_c(glyceraldehyde) - k_{dhgl}Y_c(dihydroxyacetone) \quad (3)$$

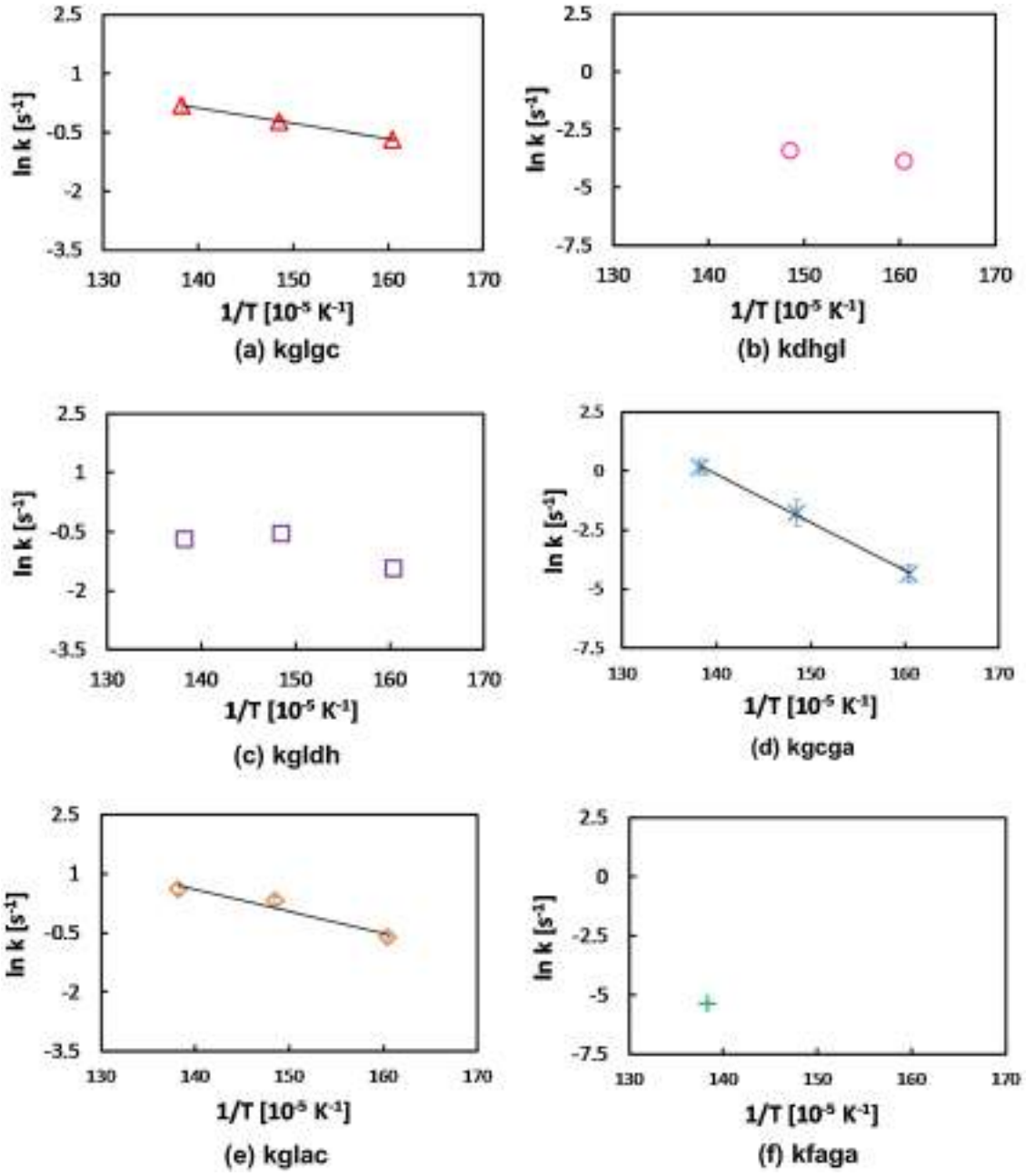

Fig. 7. Arrehenius plot of each reaction constant (experimental conditions: 300–450 °C, 25 MPa, and 0.1 wt % of glyceraldehyde). (a) kglgc, (b) kdhgl, (c) kgldh, (d) kgcga, (e) kglac, and (f) kfaga. Symbols: ▲ = k_{glgc}, ○ = k_{dhgl}, □ = k_{gldh}, ✳ = k_{gcga}, ◇ = k_{glac}, + = k_{faga}. Line in (a) is $\ln k = -3870/T + 5.5267$ ($R^2 = 0.9996$). Line in (d) is $\ln k = -20420/T + 28.449$ ($R^2 = 0.9984$). Line in (e) is $\ln k = -5580/T + 8.4189$ ($R^2 = 0.9351$).

$$\frac{dY_c(glycolaldehyde)}{dt} = \frac{2}{3}k_{glgc}Y_c(glyceraldehyde) - (k_{gcga})Y_c(glycolaldehyde) \quad (4)$$

$$\frac{dY_c(formaldehyde)}{dt} = \frac{1}{3}k_{glgc}Y_c(glyceraldehyde) - k_{foga}Y_c(formaldehyde) \quad (5)$$

$$\frac{dY_c(acetaldehyde)}{dt} = \frac{2}{3}k_{glac}Y_c(glyceraldehyde) - k_{acga}Y_c(acetaldehyde) \quad (6)$$

$$\frac{dY_c(formic\ acid)}{dt} = \frac{1}{3}k_{glac}Y_c(glyceraldehyde) - k_{faga}Y_c(formic\ acid) \quad (7)$$

$$\frac{dY_c(gas)}{dt} = k_{foga}Y_c(formaldehyde) + k_{gcga}Y_c(glycolaldehyde) + k_{acga}Y_c(acetaldehyde) + k_{faga}(formic\ acid) \quad (8)$$

Here, Y_c, t, and k denote the carbon yield of each compound [-], reaction time [s], and reaction rate constant [s^{-1}], respectively. This set of differential equations can be used to express the change in carbon yield for each compound with time. The reaction rate constants were calculated using the least squares method (LSM) to determine the best fit between the numerical calculation with the experimental data.

3.4. Decomposition products of glyceraldehyde

Fig. 6 shows the experimental data and values calculated using Eqs. (2)–(8) for glyceraldehyde at 350, 400, and 450 °C. All the compounds presented in Fig. 5 were observed, including formic acid and

Table 2
Activation energies and pre-exponential factors of radical reactions (Experimental conditions: 300–450 °C, 25 MPa, and 0.1 wt % of glyceraldehyde). 95% reliability is a reliability interval of calculation.

reactions	activation energy (kJ mol^{-1})		pre exponential factor (s^{-1})	
	Average	95 % reliability	Average	95 % reliability
glgc	3.21×10^{1}	$3.32 \times 10^{1} \pm 1.04 \times 10^{\circ}$	2.51×10^{2}	$2.55 \times 10^{2} \pm 2.25 \times 10^{1}$
glac	4.64×10^{1}	$4.56 \times 10^{1} \pm 9.87 \times 10^{\circ}$	4.53×10^{3}	$4.72 \times 10^{3} \pm 4.76 \times 10^{2}$
gcga	1.70×10^{2}	$1.75 \times 10^{2} \pm 1.71 \times 10^{1}$	2.27×10^{12}	$5.56 \times 10^{12} \pm 2.69 \times 10^{12}$

acetaldehyde, which are the products of the radical reaction. The ratio of the carbon yield of acetaldehyde to that of formic acid was almost 2. This ratio is expected when these compounds are not easily gasified.

The calculated values and the empirical data were in good agreement with each other. The kinetic rate constants for glyceraldehyde decomposition are presented in Table 1.

3.5. Effect of temperature on reaction type

To understand the effect of temperature on the reactions and to differentiate the reaction mechanisms into ionic and free radical reactions, Arrhenius plots were developed. As the temperature of the water approaches its supercritical region, the number of intermediate ions decreases and free radical reactions dominate [13,24–26]. If a reaction is ionic, decrease in the reaction rate constant should be observed in the supercritical temperature region in the Arrhenius plot due to the decrease in ion concentration. Meanwhile, if a reaction is a radical one, straight line should be obtained in the Arrhenius plot.

The Arrhenius plots of all the reactions are shown in Fig. 7. The reaction rate constants whose values were equal to zero were not included in the graph because their logarithms cannot be defined. The rate constants for retro-aldol reaction (k_{glgc}) gave a straight line in the Arrhenius plot. Thus, under hydrothermal conditions, the radical reaction was clearly the main mechanism for the retro-aldol condensation. The related reaction of glyceraldehyde to acetaldehyde and formic acid (k_{glac}) also gave a linear plot. Similarly, the gasification reactions of glycolaldehyde to gas (k_{gcga}) followed the linear Arrhenius trend. However, the isomerization reactions of glyceraldehyde to dihydroxyacetone (k_{gldh}) and dihydroxyacetone to glyceraldehyde (k_{dhgl}) were classified as ionic reactions as the corresponding graphs did not show the linear Arrhenius behavior. The decomposition of formic acid, formaldehyde, and acetaldehyde was negligible in this temperature range. The activation energy and pre-exponential factor for the radical reactions are presented in Table 2.

The Arrhenius plot of the reaction rate constants also supports our findings that the retro-aldol reaction under hydrothermal conditions occurs via a radical reaction mechanism.

It is to be noted that ionic and radical reactions in water near critical point has been discussed by previous researchers, too [27–29]. For the case of competitiveness between radical and ionic reaction, Bühler et al. [30] discussed non-Arrhenius behavior where reaction rate decreased in the vicinity of critical temperature, and then increased following Arrhenius low in the supercritical temperature region for glycerol decomposition. In this study, we observed linear increase of reaction rate in the Arrhenius plot for glyceraldehyde. This fact indicates that the effect of ionic reaction is negligible if any for the reaction studied here.

4. Conclusion

The conversion of glyceraldehyde under sub- and supercritical conditions was performed to elucidate if the mechanism of the retro-aldol condensation under hydrothermal conditions is radical or ionic. Formic acid, whose generation is explained by the radical reaction mechanism, was observed and the Arrhenius plot of the retro-aldol reaction was a straight line for both the sub- and supercritical water regions. Thus, the retro-aldol reaction of glyceraldehyde under hydrothermal conditions is a radical reaction.

Acknowledgement

RIM would like to grateful the financial support from Indonesia Endowment Fund for Education (LPDP) for PhD scholarship.

References

[1] P. McKendry, Energy production from biomass (part 1): overview of biomass, Bioresour. Technol. 83 (2002) 37–46.
[2] D. Shen, S. Yao, S. Wu, Q. Liu, R. Xiao, Kinetic study on the thermo-oxidative degradation of glyceraldehydeunder different oxygen concentrations, J. Anal. Appl. Pyrolysis 113 (2015) 665–671.
[3] T.M. Aida, Y. Sato, M. Watanabe, K. Tajima, T. Nonakaa, H. Hattori, A. Kunio, Dehydration of d-glucose in high temperature water at pressures up to 80MPa, J. Supercrit. Fluids 40 (2007) 381–388.
[4] S. Nanda, M. Gong, H.N. Hunter, A.K. Dalai, I. Gökalp, J.A. Kozinskia, An assessment of pinecone gasification in subcritical, near-critical and supercritical water, Fuel Process. Technol. 168 (2017) 84–96.
[5] A. Amrullah, Y. Matsumura, Supercritical water gasification of sewage sludge in continuous reactor, Bioresour. Technol. 249 (2018) 276–283.
[6] T. Samanmulya, S. Inoue, T. Inoue, Y. Kawai, H. Kubota, H. Munetsuna, T. Noguchi, Y. Matsumura, Gasification characteristics of alanine in supercritical water, J. Jpn. Pet. Inst. 57 (2014) 225–229.
[7] Y. Matsumura, M. Harada, D. Li, H. Komiyama, Y. Yoshida, H. Ishitani, Biomass GAsification in supercritical water with partial oxydation, J. Jpn. Inst. Energy 82 (2003) 919–925.
[8] A. Goodwin, G. Rorrer, Reaction rates for supercritical water gasification of xylose in a micro-tubular reactor, Chem. Eng. J. 163 (1–2) (2010) 10–12.
[9] Y. Gorbaty, G.V. Bondarenko, Transition of liquid water to the supercritical state, J. Mol. Liq. 239 (2017) 5–9.
[10] M.J. Antal, S. Glen Allen, D. Schulman, X. Xu, R.J. Divilio, Biomass gasification in supercritical water, Ind. Eng. Chem. Res. 39 (2000) 4040–4053.
[11] Y. Matsumura, T. Minowa, B. Potic, S. Kersten, W. Prins, W. van Swaaij, B. van de Beld, D. Elliott, G. Neuenschwander, A. Kruse, M. Antal, Biomass gasification in near- and super-critical water: status and prospects, Biomass Bioenergy 29 (4) (2005) 269–292.
[12] B. Kabyemela, T. Adschiri, R. Malaluan, K. Arai, Glucose and fructose decomposition in subcritical and supercritical water: detailed reaction pathway, mechanisms, and kinetics, Ind. Eng. Chem. Res. 38 (8) (1999) 2888–2895.
[13] C. Promdej, Y. Matsumura, Temperature effect on hydrothermal decomposition of glucose in sub- and supercritical water, Ind. Eng. Chem. Res. 50 (14) (2011) 8492–8497.
[14] T.M. Aida, N. Shiraishi, M. Kubo, M. Watanabe, R.L. Smith, Reaction kinetics of D-xylose in sub- and supercritical water, J. Supercrit. Fluids 55 (1) (2010) 208–216.
[15] A.K. Goodwin, G.L. Rorrer, Modeling of supercritical water gasification of xylose to hydrogen-rich gas in a hastelloy microchannel reactor, Ind. Eng. Chem. Res. 50 (2011) 7172–7182.
[16] N. Paksung, Y. Matsumura, Decomposition of xylose in sub- and supercritical water, Ind. Eng. Chem. Res. 54 (2015) 7604–7613.
[17] N. Paksung, R. Nagano, Y. Matsumura, Detailed mechanism of xylose decomposition in near-critical and supercritical water, Energy Fuels 30 (10) (2016) 7930–7936.
[18] M. Sasaki, M. Furukawa, K. Minami, T. Adschiri, K. Arai, Kinetics and mechanism of cellobiose Hydrolysis and Retro-Aldol Condensation in Subcritical and Supercritical Water, Ind. Eng. Chem. Res. 41 (2002) 6642–6649.
[19] T. Honma, H. Inomata, Density functional theory study of glyceraldehyde conversion in supercritical water, J. Supercrit. Fluids 90 (2014) 1–7.
[20] A. Chuntanapum, T.L.-K. Yong, S. Miyake, Y. Matsumura, Behavior of 5-HMF in subcritical and supercritical water, Ind. Eng. Chem. Res. 47 (2008) 2956–2962.
[21] Y. Lu, L. Guo, C. Ji, X. Zhang, X. Hao, Q. Yan, Hydrogen production by biomass gasification in supercritical water: a parametric study, Int. J. Hydrogen Energy 31 (7) (2006) 822–831.
[22] H. Kishida, F. Jin, X. Yan, T. Moriya, H. Enomoto, Formation of lactic acid from glycolaldehyde by alkaline hydrothermal reaction, Carbohydr. Res. 341 (2006)

2619–2623.
[23] X. Lü, S. Saka, New insights on monosaccharides' isomerization, dehydration and fragmentation in hot-compressed water, J. Supercrit. Fluids 61 (2012) 146–156.
[24] C. Promdej, A. Chuntanapum, Y. Matsumura, Effect of temperature on tarry material production of glucose in supercritical water gasification, J. Jpn. Inst. Energy 89 (12) (2010) 1179–1184.
[25] A. Kruse, E. Dinjus, Hot compressed water as reaction medium and reactant Properties and synthesis reactions, J. Supercrit. Fluids 39 (2007) 362–380.
[26] D. Shoji, K. Sugimoto, H. Uchida, K. Itatani, M. Fujie, S. Koda, Visualized kinetic aspects of decomposition of a wood block in sub- and supercritical water, Ind. Eng. Chem. Res. 44 (2005) 2975–2981.
[27] S. Ramayya, A. Brittain, C. Dealmeida, W. Mok, M. Antal, Acid-catalyzed dehydration of alcohols in supercritical water, Fuel 66 (10) (1987) 1364–1371.
[28] M. Antal, W. Mok, J. Roy, A. Raissi, D. Anderson, Pyrolytic sources of hydrocarbons from biomass, J. Anal. Appl. Pyrolysis 8 (1–4) (1985) 291–303.
[29] X. Xu, M. Antal, D. Anderson, Mechanism and temperature-dependent kinetics of the dehydration of tert-butyl alcohol in hot compressed liquid water, Ind. Eng. Chem. Res. 36 (1) (1997) 23–41.
[30] W. Buhler, E. Dinjus, H. Ederer, A. Kruse, C. Mas, Ionic reactions and pyrolysis of glycerol as competing reaction pathways in near- and supercritical water, J. Supercrit. Fluids 22 (1) (2002) 37–53.